

Figure 4. Comparison of the original and classified RS images.

- a) original Landsat TM image of 1989, b) classified TM image of 1989,  
c) original Landsat ETM image of 2001, d) classified ETM image of 2001.

For the actual classification, a supervised statistical maximum likelihood classification (MLC) has been used assuming that the training samples have the Gaussian distribution [11]. In order to define the sites for the training signature selection, from the images, two to three areas of interest (AOI) representing the forest and non-forest classes have been selected through thorough analysis using a polygon-based approach. The separability of the training signatures was firstly checked in feature space and then evaluated using transformed-divergence (TD) separability measure. The values of TD separability measure range from 0 to 2.0 and indicate how well the selected pairs are statistically separate. The values greater than 1.9 indicate that the pairs have good separability [7]. After the investigation, the samples that demonstrated the greatest separability were chosen to form the final signatures. The final signatures included about 436-583 pixels. The final classified images are shown in

Figure 4b,d. Looking at the classified images shown in Figure 4, one can observe what kind of changes had occurred in those periods in the forest cover of the Bogdkhan Mountain.

*Forest biomass mapping*

As the initial ERS SAR data were represented in a SLC format, it was necessary to generate coherence and amplitude images. The coherence images are generated by using both the amplitude and phase information from a pair of SLC images. The coherence values range between 0 and 1. If some land surface changes had occurred in a target area between the two image acquisition periods, then coherence is low and if no changes had occurred, then the coherence is high. In general, the coherence over a dense forest and shrub will be the lowest, while for the bare soil, the coherence will be the highest. After deriving the coherence and amplitude images, they were integrated with the JERS-1 SAR data. The SAR and coherence images are shown in Figure 5. Then, on the integrated image four classes indicating different biomass values have been defined. For the actual classification, Mahalanobis distance method was used and the result was reliable. The final forest biomass map is shown in Figure 6.

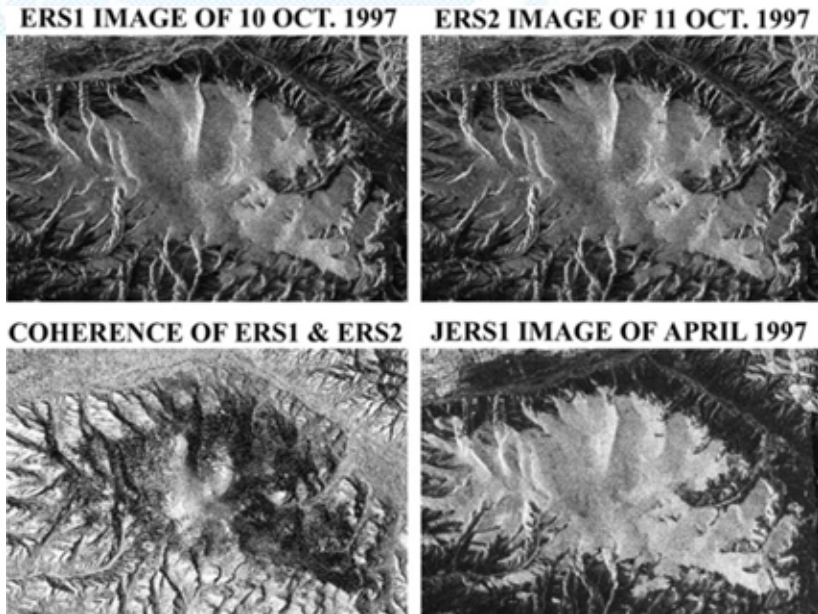


Figure 5. The SAR and coherence images.

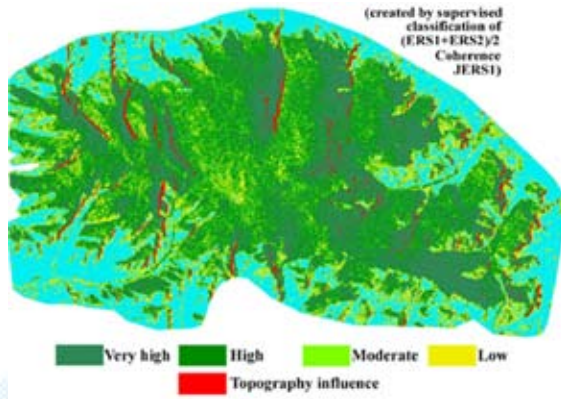


Figure 6. Forest biomass map created from the SAR images.

### 3.3. Case study-3: Pasture land degradation study and mapping at regional and local levels

Pasture land plays an important role for the Mongolian animal husbandry, because they are grazing home to over 35 million head of livestock and are used by 195,000 herding families. In recent years, the Mongolian pasture land has been seriously deteriorated and there have been different natural and socio-economic reasons on this. The severe droughts for the last few years and the growing number of livestock have been the main factors for the increased land degradation in many parts of the country. The traditional system of grazing rotation between four seasonal pastures, followed by all experienced herders, has been increasingly ignored by the new herders. Out of season grazing for example, winter reserve pastures grazed by trespassers in summer, while the habitual user is absent had become common [12]. At present, the pasture land degradation is a serious problem in Mongolia.

The aim of this research is to conduct a) a study on the pasture land degradation in Arkhangai aimag, Central Mongolia using multitemporal RS images, b) mapping of pasture land degradation using very high resolution satellite images. As data sources Landsat TM data of September 1987, Landsat ETM+ data of September 2001, topographic maps of scale 1:100.000, pasture map of scale 1:200.000, GPS measurements, ground validation data and SPOT 5 images, have been used.

#### A study on the pasture land degradation

The test site covers Jargalant, Erdene-Mandal and Tsetserleg sums

of Arkhangai aimag. By the forest-vegetation classification, the test area is included in the Khangai region and is dominated by the mixed landscapes of forest and steppe. In the isolated rural sites of the study region, it was very difficult to find accurate ground truth information related to the distribution of the winter camps of herders. Therefore, in order to conduct the thorough pastureland degradation study, we had to accurately define the precise locations of the winter camps. For this purpose, a GPS-based field survey was conducted. The Landsat TM image of the study area and the spots of the GPS measurements are shown in Figure 7.

As seen from Figure 7, the winter camps are located too close to each other (i.e. they are within 8km-10km distance from each other) and mainly built up approaching the forest sides. The reason for that is because over the past few years there have been severe droughts in the region due to which some rivers and small lakes have been dried out. Moreover, because of the droughts the vegetation covers have been degraded. As a result, in summer herding families had to move to their camps only in June or July. Meanwhile, during autumn period the hay making has been significantly reduced. Therefore, during both summer and winter seasons many herding families had to live together or closely live in good pasture areas, thus significantly degrading the pasture areas.

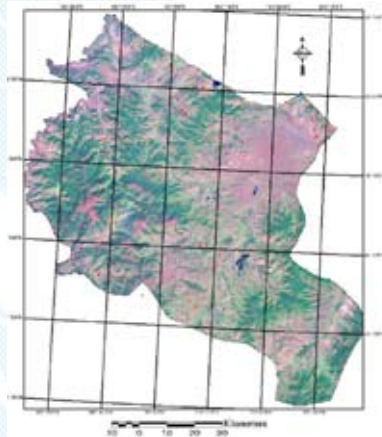


Figure 7. Landsat TM image of Jargalant, Erdene-Mandal and Tsetserleg sums of Arkhangai aimag and the spots of the GPS measurements.

To define the land degradation classes, initially, the RS images have been classified using supervised (Mahalanobis distance) and

unsupervised (isodata) classification methods. The results indicated that the supervised method performed more accurately than the supervised method (Figure 8). After the classifications, the total areas belonging to the selected classes have been calculated and the areas related to each class presented in hectares (ha) are shown in Table 1. As seen from table 1, in 1987 forest and meadow vegetation occupied 308,168ha and 173,903ha, while by 2001 they had been reduced to 298,421ha and 207,692ha, respectively. Furthermore, as seen from table 1, in 1987 the pastureland and degraded pastureland occupied 276,084ha and 116,883ha, respectively whereas in 2001 they accounted for 252.772ha and 117,533ha, accordingly. Here, the forest reduction is directly related with illegal timber preparation of the local people, while the degradation of the meadow vegetation and pasturelands are related with overgrazing and other environmental factors.

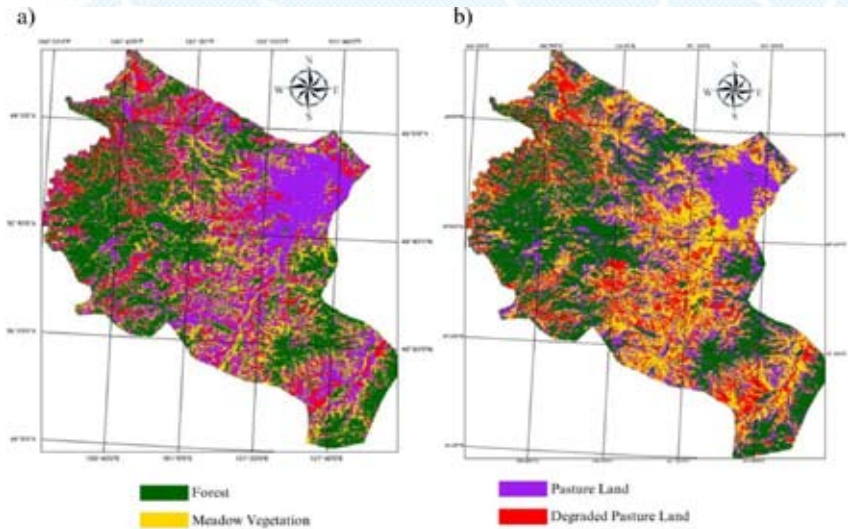


Figure 8. The classified images of Landsat TM of 1987 and Landsat ETM+ data of 2001.

Table 1. Total areas belonging to the selected classes.

Land cover types	1987	2001
Forest	308.168	298.421
Meadow Vegetation	173.903	207.692
Pasture land	276.084	252.772
Degraded pasture land	116.883	117.533

*Mapping of pasture land degradation*

The test site covers the rural area and urban buffer zone located near the capital city of Ulaanbaatar. For a large scale mapping (ie, scale of 1:5000) of pasture land degradation as well as pasture vegetation, panchromatic (2.5m) and multispectral (10m) SPOT 5 images, have been used. The SPOT 5 images of the study area are shown in Figure 9. For pasture land degradation, 3 classes (namely, high, moderate and low) have been identified based on the NDVI values of the SPOT 5 images. For pasture vegetation mapping, a visual interpretation has been applied to the created false colour images. In order to enhance the vegetation classes and their boundaries, different spectral (eg, Brovey transform, intensity-hue-saturation enhancement, etc.) and spatial enhancement (Laplacian and other high pass filters) techniques were applied to the original SPOT 5 images. The final outputs are shown in Figure 10. As seen from Figure 10, using the maps created by the use of high resolution satellite images, one can conduct very sophisticated analysis.

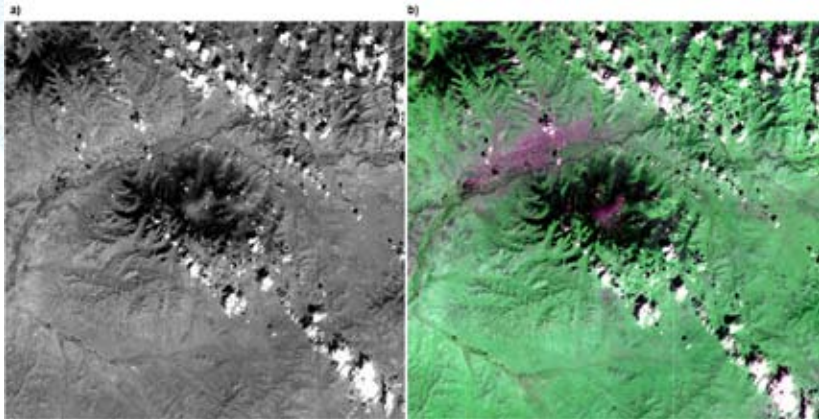


Figure 9. Panchromatic (a) and multispectral (b) SPOT 5 images of the study area.

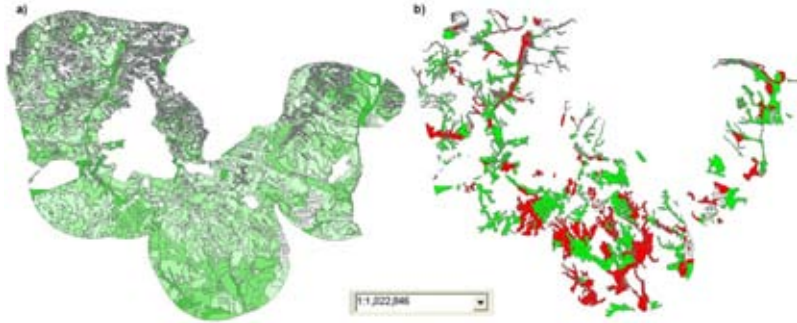


Figure 10. Pasture vegetation (a) and land degradation (b) maps created by the use of SPOT 5 images.

#### 4. Conclusions

The aim of this study was to apply some advanced techniques and technologies based on modern RS and GIS for different land degradation and desertification studies in Mongolia. For this end, three different case studies were given. The first case study described a land degradation and desertification study in Bayan soum area using a water balance model in which data sets from multiple sources were used. The second case study highlighted a forest land degradation study and forest biomass mapping in Bogdkhan Mountain using multitemporal optical and microwave satellite images with different spatial and spectral resolutions. The third case study described a pasture land degradation study and pasture vegetation mapping at regional and local levels using high and very high resolution optical RS images. Overall, the research indicated that modern techniques and technologies based on RS and GIS are reliable tools for different land degradation and desertification studies.

## 5. References

1. Amarsaikhan, D. and Sato, M., 2003, The role of high resolution satellite images for urban area mapping in Mongolia, Full paper published in the 'Reviewed Papers' part of Proceedings of the Computers for Urban Planning and Urban Management (CUPUM)'03 International Conference, Sendai, Japan, pp.1-12.
2. Amarsaikhan, D., Ganzorig, M. and Bolorchuluun, Ch., 2007, Method for restoration and conservation of abandoned crop land in Mongolia using RS and GIS, Full paper published in Proceedings of Conference on Mongolian Environmental RS, Ulaanbaatar, Mongolia.
3. Amarsaikhan, D., Narantuya, D. and Leeuw, 2008, NGIC project contribution to the environmental sustainability in Mongolia, Full paper published in Proceedings of the International Conference "Fundamental and applied issues of ecology evolutionary biology", Ulaanbaatar, Mongolia.
4. Amarsaikhan, D., Bolorchuluun, Ch., Narangerel, Z. and Gantuya, R., 2009a, Integration of RS and GIS for forest monitoring in Mongolia, Full paper published in CD-ROM Proceedings of the Asian Conference on RS, Beijing, China.
5. Amarsaikhan, D., Ganzorig, M., Blotvogel, H.H., Nergui, B. and Gantuya, R., 2009b, Integrated method to extract information from high and very high resolution RS images for urban planning, *Journal of Geography and Regional Planning*, Vol. 2(10), pp. 258-267.
6. Amarsaikhan, D., Blotvogel, H.H., van Genderen, J.L., Ganzorig, M., Gantuya, R. and Nergui, B., 2010, Fusing high resolution TerraSAR and Quickbird images for urban land cover study in Mongolia, *International Journal of Image and Data Fusion*, Vol.1, No.1, pp.83-97.
7. ERDAS, 1999, Field guide, Fifth Edition, ERDAS, Inc. Atlanta, Georgia.
8. Ganzorig, M., Batbayar, G. and Amarsaikhan, D., 2005, A study on pasture land degradation in Mongolia using RS, Full paper published in CD-ROM Proceedings of the Asian Conference on RS, Hanoi, Vietnam, pp.ALU2-2\_1-5.
9. Jetten, V., 2009, Bayan water balance model, NGIC deliverable 1.4.4, NGIC project report, pp.1-35.
10. Mather, P.M., 1999, *Computer Processing of Remotely-Sensed Images: An Introduction*, Second Edition, (Wiley, John & Sons).
11. Richards, J. A. and Jia, S., 1999, (Berlin: Springer-Verlag).
12. Sustainable Grassland Management, 2000, Project Document, Project of the Government of Mongolia and UNDP, pp.48.



## Seismic Hazard assessment of Mongolia



Sciences Council of Asia

**Dr. Ts. Batsaikhan**

*Researcher, The Research Center for Astronomy and Geophysics, Mongolia Academy of Sciences (MAS), Mongolia*

### Abstract

The geological, geomorphological, engineering-geological and hydrogeological building conditions of Ulaanbaatar town have been generalized to perform a site-specific earthquake hazard analysis. Some regular trends, such as changing in key seismic parameters with depth, were first exhibited for the area of the town. They are exhibited with regard to texture of soil, soil conditions and resolution yielded by the geophysical methods in use depending on penetration depth. Probabilistic seismic characteristics have been estimated for the grounds most typical of the upper section. The proposed technique of assessment of seismic effects with regard to probabilistic approach in detailing the initial data can be used for large-scale (1:25000 or 1:10000) mapping of seismic risk of the area of Ulaanbaatar town

Founded by nomadic population in 1639, Ulaanbaatar town became a settlement in 1778. Since that time it has been known as a large religious (Buddhism residence), administrative, and trading center. Prior to 1924 it was known as Orgo (Mongolian headquarters, thus received the name Urga in contemporary literature). In 1924, it was renamed as Ulan-Bator. Situated in the Tuul River valley (Selenga River basin), it is the capital of Mongolia with the population of more than 600 000 people at the home population of about 2.5 million people. It has most of the industrial facilities of Mongolia. The actual elevations on the town area are 1200-1500 m. Among the mountains bordering the town, the highest is Bogda uul, 2256 m, on the southern end. According to the limit prescribed in 1996, the total area of the town is about 4800 km<sup>2</sup>, 520 km of which falls on the build-up territory. The coordinates are 55° E and 47°55' N. The town is bordered by the Bogd uul massif on the south. The northern slope has a larger degree than the southern and is dissected by the deeply entrenched Zaisan, Ikh tengeriin am, Khurkhree and other creek valleys.

Earthquakes are one of the primary hostilities for the population of Ulaanbaatar as it is situated in the Mongolo-Baikal seismic zone, one of the most seismically active in the world [1]. Therefore, particular emphasis should be placed on the promotion of seismic safety of the town, that is, the compliance of the requirements of earthquake engineering and reconstruction in accordance with the predicted seismic hazard level. The solution of these problems is associated with the efforts directed towards refining of present seismic zoning techniques for the urban areas of Mongolia [2]. It has been just this research which we have made on the area of Ulaanbaatar town.

Analysis has been performed on seismic and tectonic features of the area of Ulaanbaatar town. From this analysis, we might reason that the geological, seismotectonic and statistical data on the recent earthquakes occurred in the area of Ulaanbaatar town suggest the need for the adjustment of its initial seismicity level and primarily of probability estimates that date from 1985.

Geological, geomorphologic, engineering-geological, and hydrological building conditions for Ulaanbaatar town have been specified and analyzed. The section of the Tola River valley is an example (Fig. 1).

Regular variations of the key seismic parameters were first related to depth (Fig. 2). They are represented with regard to soil conditions, texture of soils and resolution of the geophysical methods depending on penetration depth. Probable seismic characteristics have been evaluated for the most abundant upper-section grounds.

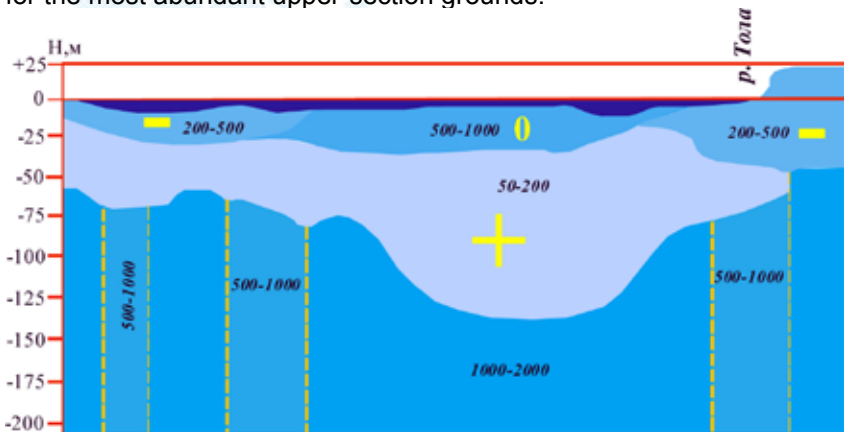


Fig. 1. Geological-geophysical section of the Tola River valley. The figures show electrical resistivities of ground layers in Ohm\*m; dashed line shows the inferred tectonic faulting; the ground layer thicknesses are variously colored.

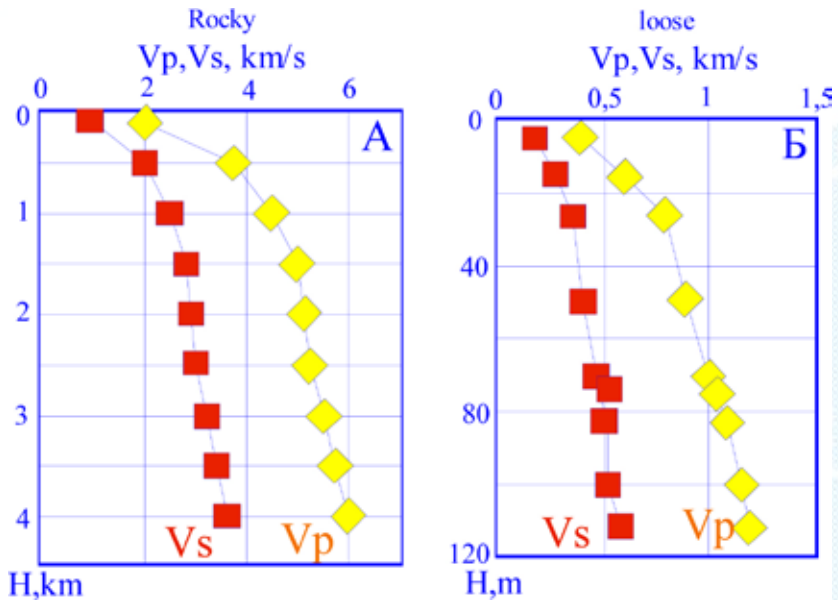


Fig. 2. Integrated data on the P- and S-wave velocity distribution in the upper earth crust adjacent to Ulaanbaatar town.

A – velocity variations in rocky grounds to 4 km.

B – velocity variations in loose grounds to 200 m.

The procedure has been substantiated and the models of two types have been constructed: for the uppermost geological section and up to depth of several kilometers. With this procedure, as applied to the models, we could perform the calculations of accelerograms, acceleration spectra and frequency characteristics and obtain a set of parameters for major seismic effects. On this basis the first-approximation sketch-map of seismic risk (peak accelerations) and resonance frequencies has been constructed for unconsolidated strata of the area of Ulaanbaatar town.

The initial seismic signal-setting mode has been developed with regard to the signal conditions and large events recorded beyond the investigated area including those recorded by the worldwide network. As a result the accelerogram has been synthesized in accordance with probable large earthquakes meeting the initial seismicity of the area (Fig. 3).

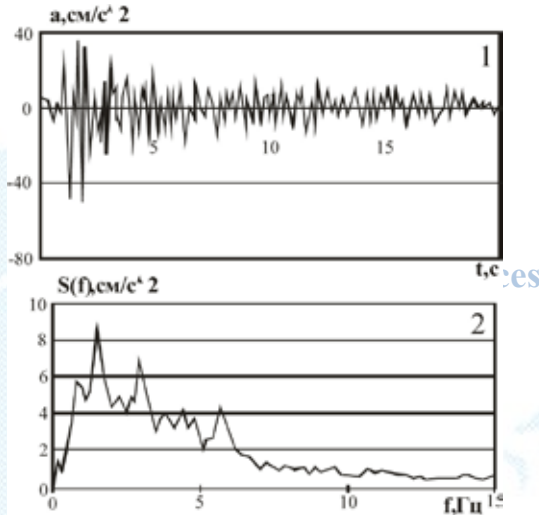


Fig. 3. Synthesized initial accelerogram (1) and its spectrum (2) for solid grounds of the area of Ulaanbaatar town.

Seismic risk probability mapping has been recently practiced in the world (including Russia). As this takes place, the expected intensity of ground shaking on the maps of general seismic zoning is presented in units of the so-called *effective acceleration* arising from the solid-ground earthquakes. The mapping of detailed zoning and microzoning consider also the influence of near-surface geological, topographical, and other local conditions. The peak accelerations are calculated for particular probability and, therefore, with regard to uncertainty with which the destructive earthquakes are expected. For the area of Ulaanbaatar (for high and particularly high building criticality rating), the initial seismicity may increase to 8 units even on condition that seismic intensity is still equal to 7 units for large-scale construction site areas.

As a result the modeling technique has been substantiated and the two-type models of the uppermost geological section have been generated to depths of several kilometers. The models differed in number of layers, layer thickness, longitudinal and transverse wave velocity layers, and absorption decrement.

The accelerograms, accelerations spectra and frequency characteristics have been calculated and a set of parameters of major seismic effects has been obtained from the substantiated techniques for the models

generated. The calculation results allow the first approximation zoning of the area of Ulaanbaatar town from the key parameters of seismic effects (Fig. 4).

The results of theoretical calculations made by the procedure developed are as follows. For the models to 12 km, both near-surface and deep-earth vertical density and velocity inhomogeneities exert some effect on the synthesized initial seismic signal whereas for the next six models only the near-surface inhomogeneities have influence on it. Accelerograms, acceleration spectra and frequency characteristics were calculated for the models.

In the first case, the accelerograms show somewhat more than twice decrement of peak accelerations in going from loose to rough and solid rocks. The degree of frequency-dependent variation was estimated by calculation of frequency characteristics. The net effect has been calculated through the division of seismic motion spectra of the surface-developed models by the initial signal spectrum. The frequency curves show a general reduction of motion intensity with overfrequency. Generally, the developed models characterize “standards” at the level of small- to large-scale seismic zoning (according to a set of parameters of seismic effects).

The near-surface section exhibits the following regularity in frequency characteristics. In thickening of loose deposits the maximums of frequency characteristics are shifted to low frequencies: from 8 Hz ( $h=10$  m) to 1.5 Hz ( $h=120$  m). The initial motions on resonance frequencies may be enhanced by loose ground layers from 4 to 6.5. As a result the accelerograms and spectra for the maximum horizontal component provide parametric characteristic of the mode of propagation throughout the area of the town.

The area of the town was first zoned from the calculated model parameters and engineering-geological and geophysical data analysis and then from the calculated parameters of seismic effects. As a result the sketch-map of seismic risk has been constructed for the area of Ulaanbaatar town showing that the maximum seismic effects for the town may vary from 40-80 to 380  $\text{cm/s}^3$  and the resonance frequencies of unconsolidated rock mass to solid rocks vary from 1.2 to 10 Hz (Fig. 4). This is the first-approximation sketch-map of real seismic effects, and the models developed have some uncertainties in the P- and S-wave velocities, interlayer thicknesses, and specific weight of the rocks. The large earthquake parameters defined for the area of Ulaanbaatar town have their variation range. Selecting calculated accelerogram cannot be unique either as it is determined by some properties typical of the